Inclusive η' production from the $\Upsilon(1S)$

M. Artuso, C. Boulahouache, S. Blusk, K. Bukin, E. Dambasuren, R. Mountain, H. Muramatsu, R. Nandakumar, T. Skwarnicki, S. Stone, and J. C. Wang
Syracuse University, Syracuse, New York 13244

A. H. Mahmood
University of Texas–Pan American, Edinburg, Texas 78539

S. E. Csorna and I. Danko
Vanderbilt University, Nashville, Tennessee 37235

G. Bonvicini, D. Cinabro, M. Dubrovin, and S. McGee
Wayne State University, Detroit, Michigan 48202

A. Bornheim, E. Lipeles, S. P. Pappas, A. Shapiro, W. M. Sun, and A. J. Weinstein
California Institute of Technology, Pasadena, California 91125

R. A. Briere, G. P. Chen, T. Ferguson, G. Tatishvili, and H. Vogel
Carnegie Mellon University, Pittsburgh, Pennsylvania 15213

N. E. Adam, J. P. Alexander, K. Berkelman, V. Boisvert, D. G. Cassel, P. S. Drell, J. E. Duboscq, K. M. Ecklund, R. Ehrlich, R. S. Galik, L. Gibbons, B. Gittelman, S. W. Gray, D. L. Hartill, B. K. Heltsley, L. Hsu, C. D. Jones, J. Kandaswamy, D. L. Kreinick, A. Magerkurth, H. Mahlke-Krüger, T. O. Meyer, N. B. Mistry, J. R. Patterson, D. Peterson, J. Pivarski, S. J. Richichi, D. Riley, A. J. Sadoff, H. Schwarthoff, M. R. Shepherd, J. G. Thayer, D. Urner, T. Wilksen, A. Warburton, and M. Weinberger
Cornell University, Ithaca, New York 14853

S. B. Athar, P. Avery, L. Breva-Newell, V. Potlia, H. Stoeck, and J. Yelton
University of Florida, Gainesville, Florida 32611

K. Benslama, B. I. Eisenstein, G. D. Gollin, I. Karliner, N. Lowrey, C. Plager, C. Sedlack, M. Selen, J. J. Thaler, and J. Williams
University of Illinois, Urbana-Champaign, Illinois 61801

K. W. Edwards
Carleton University, Ottawa, Ontario, Canada K1S 5B6
and the Institute of Particle Physics, Canada M5S 1A7

R. Ammar, D. Besson, and X. Zhao
University of Kansas, Lawrence, Kansas 66045

S. Anderson, V. V. Frolov, D. T. Gong, Y. Kubota, S. Z. Li, R. Poling, A. Smith, C. J. Stepaniak, and J. Urheim
University of Minnesota, Minneapolis, Minnesota 55455

Z. Metreveli, K. K. Seth, A. Tomaradze, and P. Zweber
Northwestern University, Evanston, Illinois 60208

S. Ahmed, M. S. Alam, J. Ernst, L. Jian, M. Saleem, and F. Wappler
State University of New York at Albany, Albany, New York 12222

K. Arms, E. Eckhart, K. K. Gan, C. Gwon, K. Honscheid, D. Hufnagel, H. Kagan, R. Kass, T. K. Pedlar, E. von Toerne, and M. M. Zoeller
Ohio State University, Columbus, Ohio 43210

H. Severini and P. Skubic
University of Oklahoma, Norman, Oklahoma 73019

S. A. Dytman, J. A. Mueller, S. Nam, and V. Savinov
University of Pittsburgh, Pittsburgh, Pennsylvania 15260

S. Chen, J. W. Hinson, J. Lee, D. H. Miller, V. Pavlunin, E. I. Shibata, and I. P. J. Shipsey
Purdue University, West Lafayette, Indiana 47907

D. Cronin-Hennessy, A. L. Lyon, C. S. Park, W. Park, J. B. Thayer, and E. H. Thorndike
University of Rochester, Rochester, New York 14627

T. E. Coan, Y. S. Gao, F. Liu, Y. Maravin, and R. Stroynowski
Southern Methodist University, Dallas, Texas 75275

(CLEO Collaboration)
(Received 11 November 2002; published 17 March 2003)

Using the CLEO II detector at CESR, we measure the η' energy spectra in $\Upsilon(1S)$ decays that we compare with models of the $\eta' g^* g$ form factor. This form factor, especially at large η' energies, may provide an explanation of the large rate for $B \to X_s \eta'$. Our data do not support a large anomalous coupling at higher q^2 and thus the large η' rate remains a mystery, possibly requiring a non-standard-model explanation.

DOI: 10.1103/PhysRevD.67.052003 PACS number(s): 13.25.Gv, 13.25.Hw, 13.66.Bc

I. INTRODUCTION

There are several interesting, unexplained phenomena in B decays. First of all, the total production of charm and charmonium seems about 10% low [1], especially when coupled with a B semileptonic branching ratio of $(10.4 \pm 0.3)\%$ [2]. Second, CLEO observed a very large rate of η' in the momentum range from 2 to 2.7 GeV/c with a branching fraction of $(6.2 \pm 1.6 \pm 1.3^{+0.0}_{-1.5}) \times 10^{-4}$ [3]. The BABAR experiment has confirmed this large rate [4]. The production of η' mesons is believed to occur dominantly via the $b \to sg$ mechanism, as strongly suggested by observation of the two-body decay $B \to \eta' K$. One explanation of the large η' rate is that the $b \to sg$ rate is not 1% as expected in the standard model, but is enhanced by new physics to be at the 10% level. This would also explain the charm deficit problem.

An alternative explanation is that of an anomalously strong coupling between the η' and two gluons [5–7]. The process $b \to sg$ followed by the two gluon coupling to the η' is shown in Fig. 1.

Experimentally, the hadronic mass associated with X_s sometimes is a K, $\sim 10\%$, and even more rarely a K^*, $\sim 1\%$; in fact, most of the rate has the mass of the X_s system larger than 1.8 GeV. Since the η' is mostly the flavor singlet η_1, as the η-η' mixing angle is between $10° - 20°$, the effective $\eta' g^* g$ coupling can be written as [8]

$$H(q^2) \varepsilon_{\alpha\beta\mu\nu} q^\alpha k^\beta \varepsilon_1^\mu \varepsilon_2^\nu, \tag{1}$$

where $q = p_b - p_s$ is the four-momentum of the virtual hard gluon (g^*), k is the four-momentum of the soft "on-shell" gluon (g), and $H(q^2)$ is the $g^* g \eta'$ transition form factor.

Chen and Kagan [8] have shown that the region of the q^2 relevant in the process $b \to sg\eta'$ can also be accessed in high energy η' production in $\Upsilon(1S)$ decay. Thus constraints can be put on the $H(q^2)$ from the η' spectrum in $\Upsilon(1S) \to ggg$ decays. $H(0)$ is found from the rate of $J/\psi \to \gamma\eta'$ decays as ~ 1.8 GeV^{-1}.

Three choices for the form factor shape $H(q^2)$ are shown in Fig. 2: (a) a slowly falling form factor from Hou and Tseng [6], $H(q^2) = 2.1$ GeV$^{-1} \alpha_s(q^2)/\alpha_s(m^2_{\eta'})$; (b) a rapidly falling form factor representative of perturbative QCD calculations, $H(q^2) = 1.7$ GeV$^{-1} m^2_{\eta'}/(q^2 - m^2_{\eta'})$ at $q^2 > 1$ GeV^2; (c) an intermediate example with $H(q^2) \propto 1/(q^2$

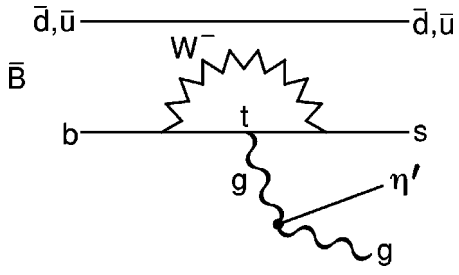

FIG. 1. Diagram for $b \to sg\eta'$.

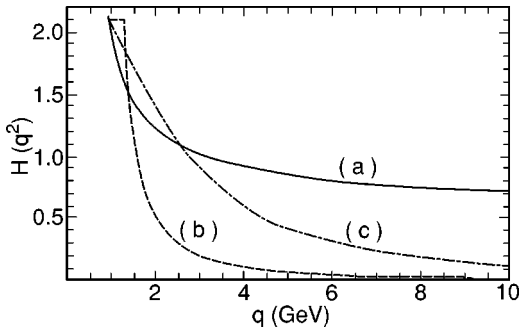

FIG. 2. Three choices for the form factor $H(q^2)$ plotted against $\sqrt{q^2}$: (a) the slowly falling form factor, (b) a rapidly falling form factor representative of perturbative QCD calculations, and (c) an intermediate example (adapted from Ref. [8]).

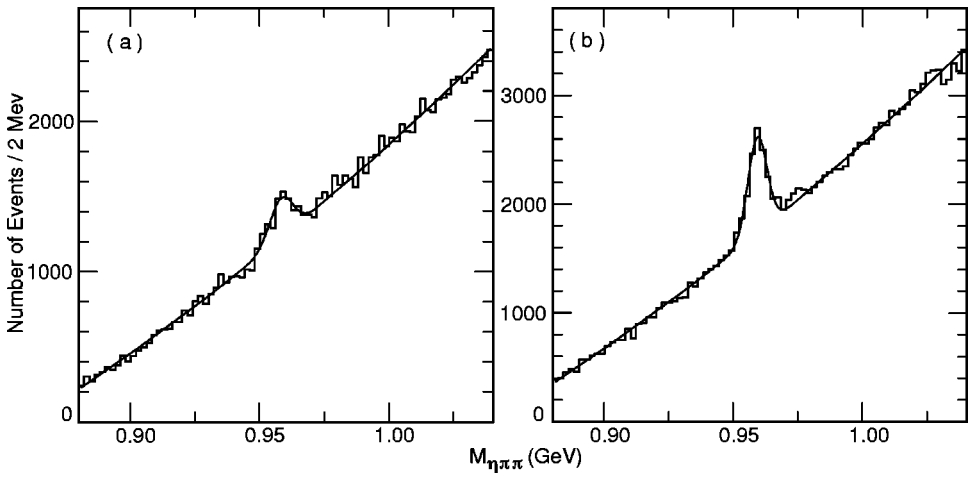

FIG. 3. The $\eta\pi^+\pi^-$ invariant mass spectrum reconstructed from $\Upsilon(1S)$ data (left), and off resonance data at 10.52 GeV (right) fit with Gaussian functions for signal and second order polynomials for background.

$+2.2^2$ GeV^2) [8]. In (b) and (c) the form factor at $q^2 \approx m_{\eta'}^2$ has been matched onto the value given in (a), which is fixed by the QCD anomaly [6]. The parametrization of the form factor in (b) follows from a simple model in which the η' is coupled perturbatively to two gluons through quark loops [7]. With the choice $H(0)=1.7$ GeV^{-1} it compares well with the perturbative QCD form factors obtained by other authors [9,10].

We will compare the theoretical predictions for $H(q^2)$ with data taken on the $\Upsilon(1S)$ resonance with the CLEO II

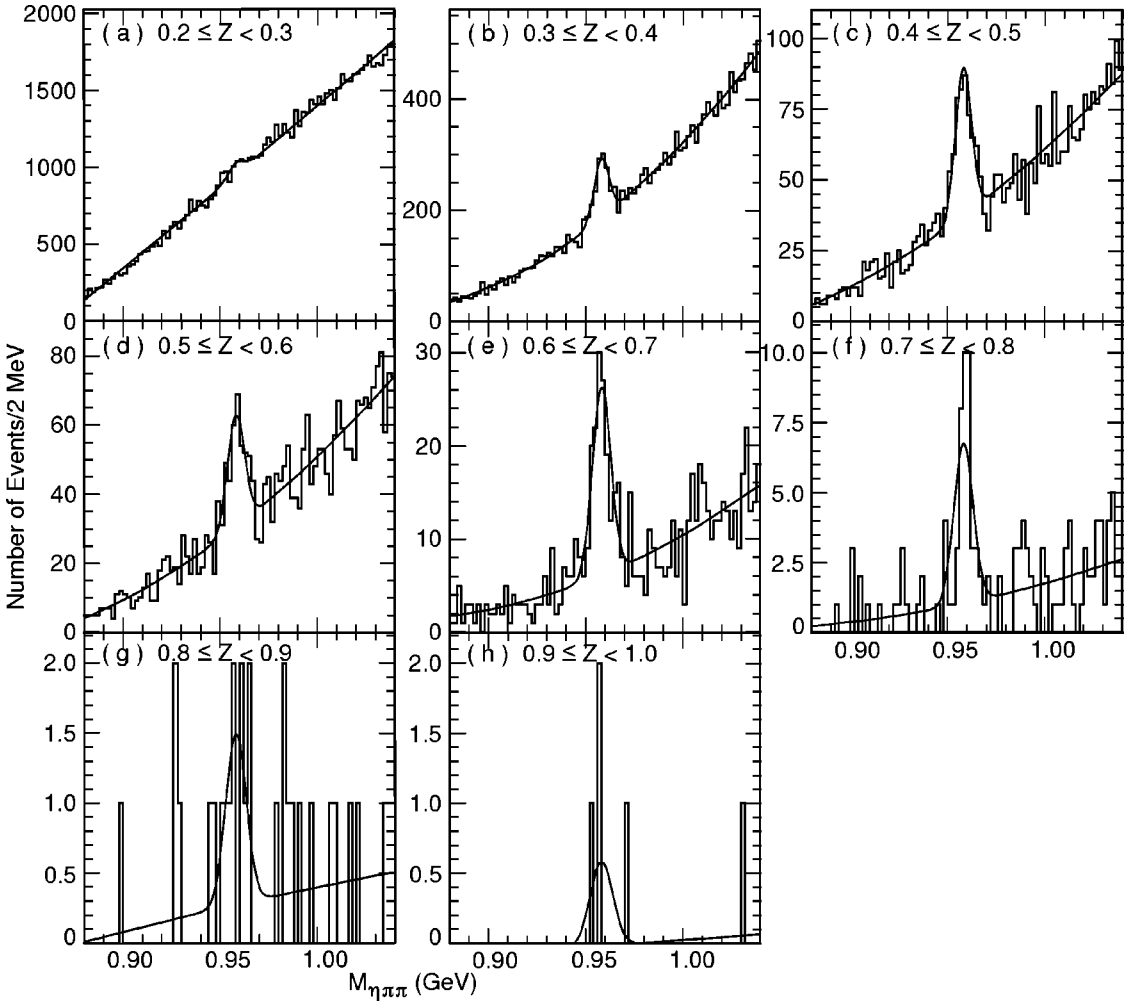

FIG. 4. The $\eta\pi^+\pi^-$ invariant mass spectra in different Z ranges reconstructed from $\Upsilon(1S)$ data, fit with a Gaussian function for signal and a second order polynomial for background.

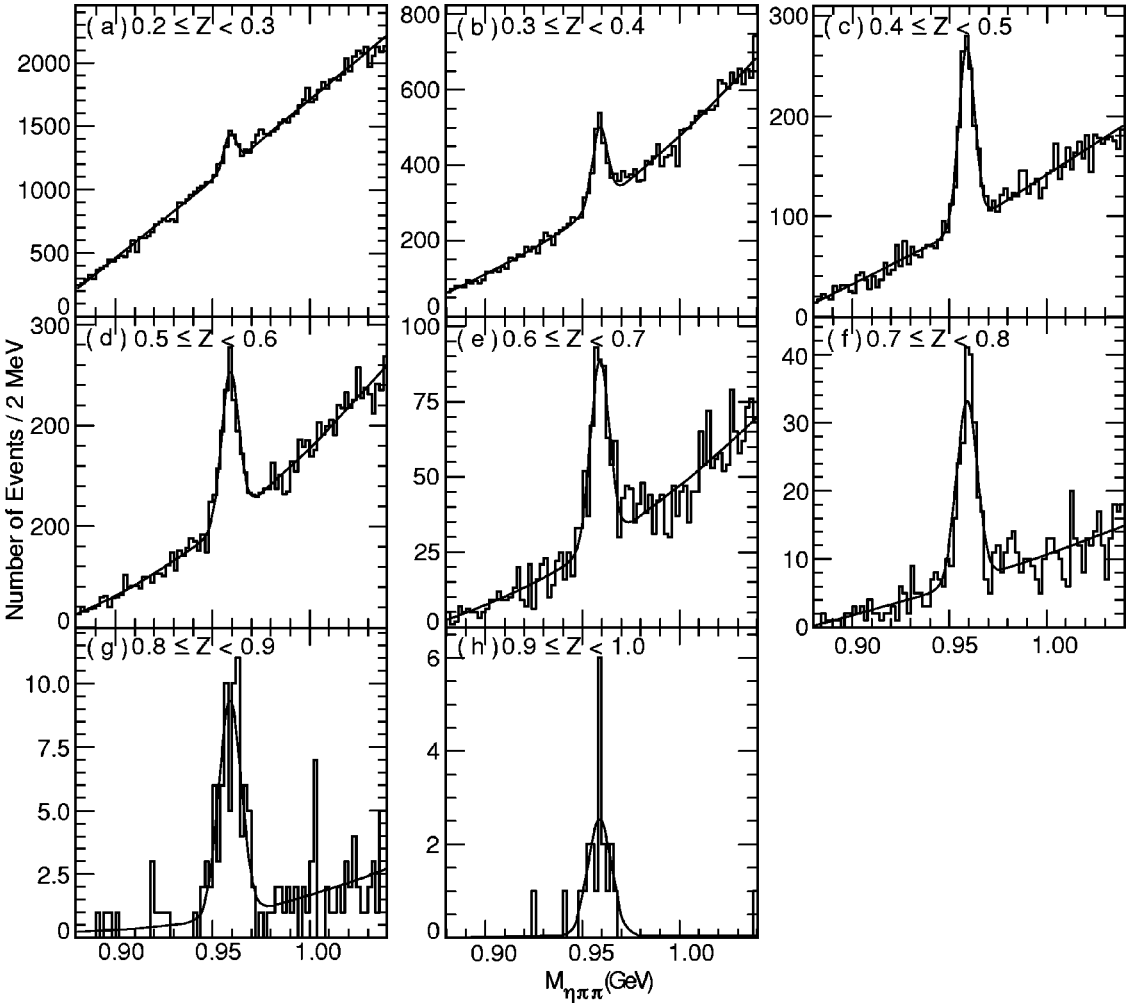

FIG. 5. The $\eta\pi^+\pi^-$ invariant mass spectra in different Z ranges reconstructed from off-resonance data, fit with a Gaussian function for signal and a second order polynomial for background.

detector at the CESR storage ring. Some information on this topic has been extracted by Kagan from ARGUS data [11].

II. DATA SAMPLE AND ANALYSIS METHOD

In this study we use 80 pb^{-1} of CLEO II data recorded at the $\Upsilon(1S)$ resonance (9.46 GeV), containing 1.862×10^6 $\Upsilon(1S)$ events. We also use off-resonance continuum data collected below the $\Upsilon(4S)$ resonance (10.52 GeV) with a total integrated luminosity of 1193 pb^{-1}.

The theoretical predictions referred to in this paper are made for $\Upsilon(1S)$ decays into three gluons (*ggg*). In order to compare our measurement to them we have to correct for the

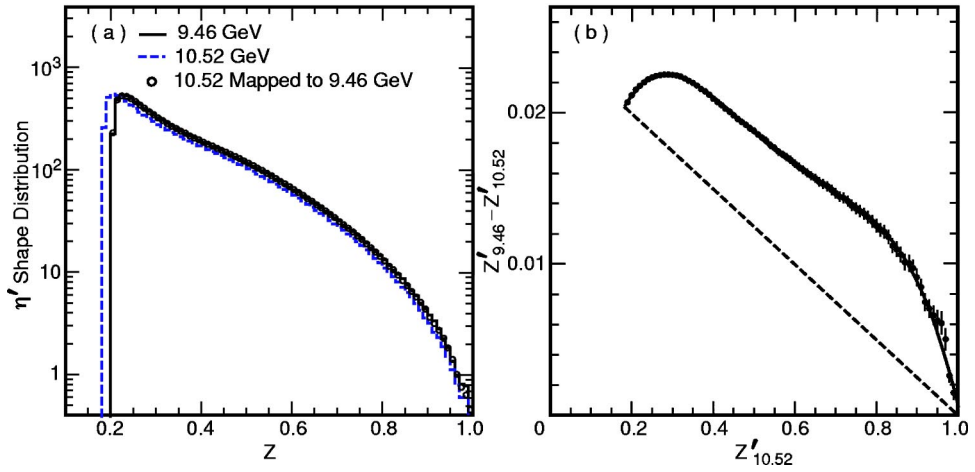

FIG. 6. (a) The $Z=E_{\eta'}/E_{\rm beam}$ distributions from Monte Carlo simulation. The solid line is the $Z=E_{\eta'}/E_{\rm beam}$ spectrum for an energy of 9.46 GeV, the dashed line is the spectrum for 10.52 GeV and the open circles are the mapped spectrum from 10.52 GeV. (b) The data points show the difference in the Z values at 9.46 and 10.52 GeV as a function of the Z value at 10.52 GeV. The solid curve is a fit to a fourth order polynomial. The dotted line shows the mapping of the linear conversion.

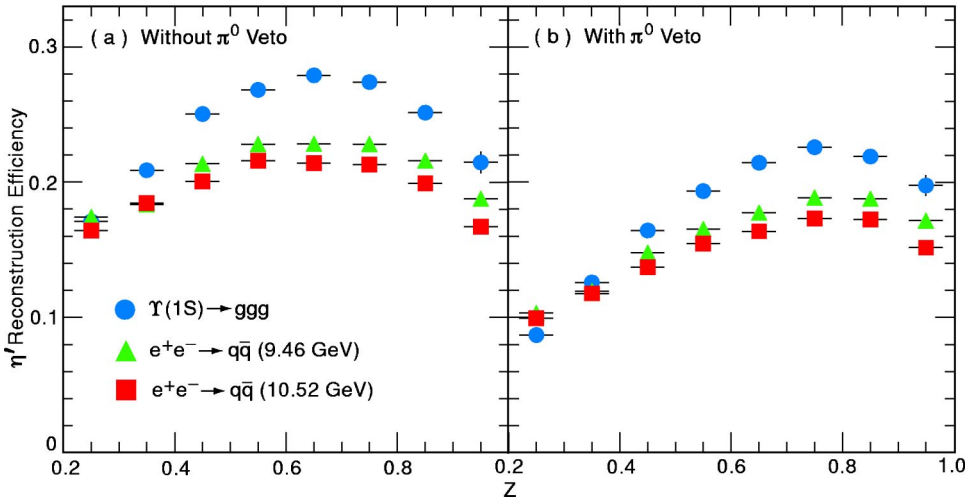

FIG. 7. The η' reconstruction efficiencies as function of Z for different MC samples (a) without a π° veto and (b) with a π° veto in the photon selection.

$\Upsilon(1S)\to\gamma^*\to q\bar{q}$ contribution, whose size is given by

$$\mathcal{B}(\Upsilon(1S)\to\gamma^*\to q\bar{q}) = R\cdot\mathcal{B}(\Upsilon(1S)\to\mu^+\mu^-) = (8.8\pm0.3)\%, \quad (2)$$

where $R_{\sqrt{s}\approx 9.5}=3.56\pm0.07$ [12] and the $\mathcal{B}(\Upsilon(1S)\to\mu^+\mu^-)$ is taken as $(2.48\pm0.06)\%$ [2].

Although several processes can contribute to inclusive η' production in $\Upsilon(1S)$ decays, it is believed that the soft processes including fragmentation populate only the low q^2 or equivalently the low Z region, where

$$Z\equiv E_{\eta'}/E_{\rm beam}=2E_{\eta'}/M(\Upsilon(1S)). \quad (3)$$

Thus in the large Z region significant η' production would indicate a large $\eta' g^* g$ coupling.

The CLEO II detector, described in detail elsewhere [13] had a high resolution electromagnetic calorimeter comprised of 7800 CsI crystals surrounding a precision tracking system. We detect η' mesons using the decay channel: $\eta'\to\eta\pi^+\pi^-$ with a branching fraction of 44%, and $\eta\to\gamma\gamma$ with a branching fraction of 39%. We identify single photons based on their shower shape and the nonproximity of charged tracks. Those photon pairs within the ''good barrel'' region of the detector, $|\cos\theta|<0.707$ (where θ is the angle with respect to the beam), that have invariant masses consistent with the η mass within 3 standard deviations are constrained to have the invariant mass of the η. For η mesons coming from low energy η' candidates ($Z<0.5$) the background from π° decay is large, and thus the candidate photons are also required not to be from a possible π° decay. We then add two opposite sign pions and form the $\eta\pi^+\pi^-$ invariant mass.

The $\eta\pi^+\pi^-$ invariant mass spectra are shown in Fig. 3 for $\Upsilon(1S)$ and for off-resonance continuum data. The spectra are fit with a Gaussian function for signal and second order polynomial function for background. The numbers of reconstructed η' are extracted from the fit. We find 1486 ± 137 η' from the $\Upsilon(1S)$ data, and 4062 ± 174 η' from the off-resonance data.

To measure the energy spectrum we reconstruct η' candidates in Z intervals. We choose the Z steps as 0.1. The invariant mass spectra are fit with the same functional form as used for Fig. 3. Here we fix the mass of the η' to our average value over all Z; the Monte Carlo simulation shows that the mass measurement should be independent of η' energy. We extract the width of the signal Gaussian distribution from Monte Carlo simulation for each Z bin and perform a smooth fit as a function of Z. The smoothed values are used in the fit as fixed parameters. The $\eta\pi^+\pi^-$ Z dependent mass spectra are shown in Figs. 4 and 5 for $\Upsilon(1S)$ and off-resonance data, respectively.

In order to extract decay rates we need to correct our raw event yields by efficiencies. These may not be equal for different intermediate states, i.e., $q\bar{q}$ versus ggg. The hadronic events at $\Upsilon(1S)$ energy arise from different sources: about 4 nb is $q\bar{q}$ from continuum e^+e^- collisions, about 2 nb from $\Upsilon(1S)\to\gamma^*\to q\bar{q}$, 18 nb from ggg, and 0.5 nb from γgg from the $\Upsilon(1S)$. The first two have same event topology and reconstruction efficiencies. We use the $q\bar{q}$ Monte Carlo generator to simulate these events. The γgg events are similar to that of ggg and have a relatively small cross section; thus we treat them the same way as ggg events. We use the ggg Monte Carlo generator to simulate this part.

We rely on off-resonance continuum data to estimate the

TABLE I. Number of reconstructed η' from $\Upsilon(1S)$ and off-resonance data and the breakdown categories of $\Upsilon(1S)$ data. Also listed are for samples with $Z>0.7$.

Sample	All Z	Z>0.7
$\Upsilon(1S)$ data	1494 ± 120	46.0 ± 8.1
off-resonance	4294 ± 130	257.1 ± 17.3
$\Upsilon(1S)\to ggg$	972 ± 120	13.9 ± 8.1
$\Upsilon(1S)\to q\bar{q}$	173 ± 5	10.6 ± 0.7
Continuum $q\bar{q}$	349 ± 11	21.5 ± 1.4
$\Upsilon(1S)\to ggg, q\bar{q}$	1145 ± 120	24.5 ± 8.1

TABLE II. Branching fractions of $\Upsilon(1S)$ to η' mesons, for all decays, three gluon decays and quark-antiquark decays for the entire η' energy spectrum and for $Z>0.7$. The errors after the values give the statistical and systematic uncertainties, respectively.

Mode	All Z	Z>0.7
$\mathcal{B}(\Upsilon(1S)\to\eta' X)$	$(2.8\pm0.4\pm0.2)\%$	$(3.1\pm0.9\pm0.3)\times10^{-4}$
$\mathcal{B}(\Upsilon(1S)\to ggg\to\eta' X)/\mathcal{B}(\Upsilon(1S)\to ggg)$	$(2.8\pm0.5\pm0.2)\%$	$(1.9\pm1.1\pm0.2)\times10^{-4}$
$\mathcal{B}(\Upsilon(1S)\to q\bar{q}\to\eta' X)/\mathcal{B}(\Upsilon(1S)\to q\bar{q})$	$(4.2\pm0.2\pm0.4)\%$	$(16.8\pm1.1\pm1.7)\times10^{-4}$

$q\bar{q}$ contribution in $\Upsilon(1S)$ data. However, the continuum data were taken for continuum subtraction in $\Upsilon(4S)$ studies. The center of mass (c.m.) energy (10.52 GeV) is close to $\Upsilon(4S)$ mass (10.58 GeV), but more than 1 GeV higher than $\Upsilon(1S)$ mass (9.46 GeV). The difference of reconstruction efficiency due to this energy difference is not negligible. We thus use different $q\bar{q}$ simulations for continuum data and $\Upsilon(1S)$ data.

The energy difference also affects the Z spectrum of η' from continuum Monte Carlo as shown in Fig. 6(a). The solid line is the $E_{\eta'}/E_{\rm beam}$ distribution for the $\Upsilon(1S)$ data (9.46 GeV) and dashed line for the continuum data (10.52 GeV). The low limits are 0.202 and 0.182, respectively. The discrepancy is significant, especially at low energy. In order to use our continuum data at 10.52 GeV we need to map it to 9.46 GeV. To do so we rely on the continuum Monte Carlo. We take the two Monte Carlo η' shape distributions at 10.52 and 9.46 GeV, denoted by $\mathcal{P}_{10.52}(z)$ and $\mathcal{P}_{9.46}(z)$ and numerically integrate them to satisfy the relation

$$\int_0^{Z'_{10.52}}\mathcal{P}_{10.52}(z)dz=\int_0^{Z'_{9.46}}\mathcal{P}_{9.46}(z)dz, \tag{4}$$

where $Z'_{10.52}$ is fixed and a value for $Z'_{9.46}$ is determined. The data points on Fig. 6(b) show the difference in $Z'_{9.46}-Z'_{10.52}$ as a function of $Z'_{10.52}$ (or equivalently Z_0 in following function). We fit the points with a fourth order polynomial function to define the mapping analytically as

$$Z=-0.215\times10^{-2}+1.2238\ Z_0-0.6879\ Z_0^2+0.8277\ Z_0^3 -0.3606\ Z_0^4. \tag{5}$$

The simplest mapping would be a linear conversion $Z=0.025+0.975\times Z_0$, shown as dotted line in Fig. 6(b). We use this alternative to estimate the systematic uncertainty due to the mapping.

That this mapping works is demonstrated in Fig. 6(a), where the spectra shown as open circles is the mapped spectrum according to Eq. (5). It overlaps well with the Monte Carlo spectrum generated at 9.46 GeV.

The η' production rate is smaller at 9.46 GeV because of less available energy. From the $q\bar{q}$ generator we found that the production rate is 93.6% that of 10.52 GeV. This factor is also considered in estimation of the η' production from $q\bar{q}$ events.

The mapping for continuum data is derived from the model-dependent Monte Carlo spectrum. If the real data and the Monte Carlo are very different then the systematic uncertainty due to this mapping could be large. To check this, we compared the measured $E_{\eta'}/E_{\rm beam}$ spectrum with the generated spectrum. Fortunately, the spectra agree reasonably well and the systematic uncertainty due to this source is negligible.

We now turn to estimating the detection efficiencies. Shown in Fig. 7 are the efficiencies estimated with different models and different energies for (a) without the π° veto and (b) with the π° veto. In the real data we applied π° veto to η' candidates with $Z<0.5$. Comparing with the efficiency from 9.46 GeV $q\bar{q}$ events, the efficiency from ggg events is roughly 15% higher, and the efficiency from 10.52 GeV $q\bar{q}$ events is roughly 7% lower. The main source of such difference is the event shape. The ggg events are more spherical while the higher energy $q\bar{q}$ events are more jetty.

III. EXTRACTION OF THE η' SPECTRUM FROM $\Upsilon(1S)$ DECAYS

The $\Upsilon(1S)$ data sample can be broken down into three parts as described in the previous section:

$$N_{\rm all}=N_{\Upsilon(1S)\to ggg}+N_{\Upsilon(1S)\to q\bar{q}}+N_{e^+e^-\to q\bar{q}}.$$

The first one has different reconstruction efficiencies from the other two. For the contribution from continuum (e^+e^-

TABLE III. The systematic uncertainties (in %) from different sources on the branching fraction measurements for the 3 gluon sample for $Z>0.7$, the $q\bar{q}$ sample, and both the 3 gluon sample for all Z and the total $\Upsilon(1S)$ sample.

Sources	$ggg(Z>0.7)$	$q\bar{q}$	All others
Reconstruction efficiency of $\pi^\pm$	4.4	4.4	4.4
Reconstruction efficiency of η	5	5	5
Number of η' from fit	2	2	2
Total number of $\Upsilon(1S)$	2.4	2.4	2.4
$\mathcal{B}(\eta'\to\pi^+\pi^-\eta)$	3.4	3.4	3.4
$\mathcal{B}(\Upsilon(1S)\to q\bar{q})$[a]		3.2	
Ratio of integrated luminosity [15]	2.9	1	
$\sigma_{\Upsilon(1S)\to\mu^+\mu^-}$	3.6	4	
Z mapping	6	3	3
Total	11	10	8.6

[a]We use $\mathcal{B}(\Upsilon(1S)\to(q\bar{q}))=(8.83\pm0.28)\%$.

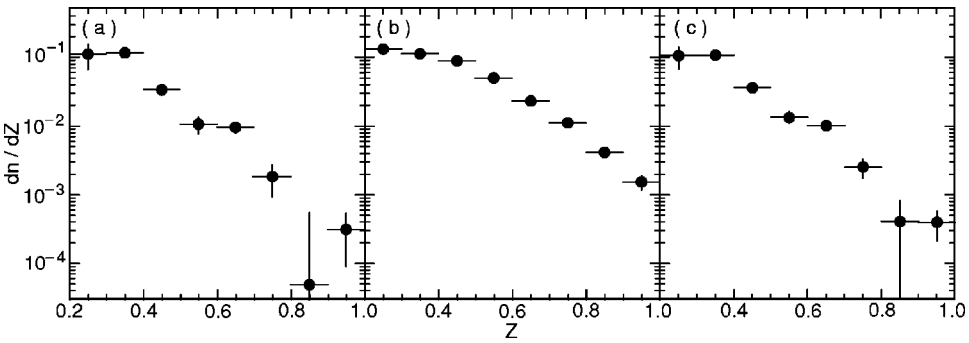

FIG. 8. The differential branching fraction dn/dZ as defined in context for (a) $\Upsilon(1S) \rightarrow ggg \rightarrow \eta' X$, (b) $\Upsilon(1S) \rightarrow q\bar{q} \rightarrow \eta' X$, and (c) $\Upsilon(1S) \rightarrow \eta' X$.

$\rightarrow q\bar{q}$) events, we multiply the number from off-resonance events at 10.52 GeV, mapped using Eq. (5), by a factor $f_{e^+e^- \rightarrow q\bar{q}}$ defined as

$$N(\eta')_{e^+e^- \rightarrow q\bar{q}}(9.46\ \text{GeV}) = N(\eta')_{e^+e^- \rightarrow q\bar{q}}(10.52\ \text{GeV}) \times f_{e^+e^- \rightarrow q\bar{q}}, \quad (6)$$

where

$$f_{e^+e^- \rightarrow q\bar{q}} = \frac{80.4}{1193} \times \frac{1/9.46^2}{1/10.52^2} \times 0.9356 \times \frac{\epsilon_{9.46}}{\epsilon_{10.52}} = 0.078 \times \frac{\epsilon_{9.46}}{\epsilon_{10.52}}, \quad (7)$$

where the first factor is the relative luminosities, the second the energy squared dependence of the cross section, the third the relative η' yield and ϵ is the Z-dependent reconstruction efficiency for $q\bar{q}$ events as shown Fig. 7.

We also want to evaluate the yield from $\Upsilon(1S) \rightarrow \gamma^* \rightarrow q\bar{q}$. Since we know that $\sigma_{\Upsilon(1S) \rightarrow \mu^+\mu^-} = 0.555 \pm 0.022$ nb and $\sigma_{e^+e^- \rightarrow \mu^+\mu^-}(9.46\ \text{GeV}) = 1.12$ nb [14], we derive the factor to be used in the $N_{\Upsilon(1S) \rightarrow q\bar{q}}$ estimation as

$$f_{\Upsilon(1S) \rightarrow q\bar{q}} = f_{e^+e^- \rightarrow q\bar{q}} \times \frac{R \cdot \sigma_{\Upsilon(1S) \rightarrow \mu^+\mu^-}}{R \cdot \sigma_{e^+e^- \rightarrow \mu^+\mu^-}} = 0.0387 \times \frac{\epsilon_{9.46}}{\epsilon_{10.52}}. \quad (8)$$

In Table I we list the number of reconstructed η' over all Z and in the high Z region for various $\Upsilon(1S)$ and continuum yields (only statistical errors are shown). Note that the total numbers of signal from $\Upsilon(1S)$ data and off-resonance data in this table are the sum of all Z bins derived bin per bin, as we need to use Z-dependent efficiencies.

The measured $\Upsilon(1S) \rightarrow \eta' X$ branching fractions are listed in Table II both for $Z > 0.7$ and for all Z. In the large Z region for 3 gluon decays, we do not have a statistically significant signal and thus derive a 90% confidence level upper limit of $\mathcal{B}[\Upsilon(1S) \rightarrow ggg \rightarrow \eta' X]_{Z>0.7} / \mathcal{B}[\Upsilon(1S) \rightarrow ggg] < 3.4 \times 10^{-4}$. We describe the systematic errors below.

The sources of systematic uncertainties are listed in Table III along with estimates of their sizes. The total systematic errors on branching ratios are $\pm 10\%$ for $q\bar{q}$ sample (independent of Z), $\pm 11\%$ for ggg sample at $Z > 0.7$, and $\pm 8.6\%$ for the rest.

We also measure the differential branching fractions as a function of Z as shown in Fig. 8. In these plots only the statistical error is shown, which dominates the total error.

We define three relevant differential branching ratio's dn/dZ as

$$\frac{dn(ggg)}{dZ} = \frac{d\mathcal{B}[\Upsilon(1S) \rightarrow ggg \rightarrow \eta' X]}{dZ \times \mathcal{B}[\Upsilon(1S) \rightarrow ggg]},$$

$$\frac{dn(q\bar{q})}{dZ} = \frac{d\mathcal{B}[\Upsilon(1S) \rightarrow q\bar{q} \rightarrow \eta' X]}{dZ \times \mathcal{B}[\Upsilon(1S) \rightarrow q\bar{q}]},$$

$$\frac{dn(1S)}{dZ} = \frac{d\mathcal{B}[\Upsilon(1S) \rightarrow \eta' X]}{dZ}. \quad (9)$$

TABLE IV. Differential branching fractions of η' ($\times 10^{-5}$). The last two rows are total branching fractions. The branching fractions in columns 2 and 3 are normalized to the total branching fraction of $\Upsilon(1S) \rightarrow (ggg)$ and $\Upsilon(1S) \rightarrow (q\bar{q})$, respectively, while the last column is normalized to all $\Upsilon(1S)$ decay. The errors are statistical only, the systematic errors on the absolute normalization for column 1 is 8.6% for $Z < 0.7$, 11% for $Z > 0.7$, and 10 and 8.6% for columns 2 and 3, respectively.

Z	$\Upsilon(1S) \rightarrow (ggg)$	$\Upsilon(1S) \rightarrow (q\bar{q})$	All $\Upsilon(1S)$
0.2–0.3	11164±4471	13205±1253	10503±3740
0.3–0.4	11624±1314	11250±685	10716±1099
0.4–0.5	3381±558	8898±416	3614±467
0.5–0.6	1067±300	5030±272	1336±251
0.6–0.7	963±181	2321±166	1011±151
0.7–0.8	184±92	1116±102	252±77
0.8–0.9	5±50	415±59	41±42
0.9–1.0	31±22	153±36	40±19
0.7–1.0	19±11	168±11	31±9
sum of all	2842±471	4239±153	2751±394

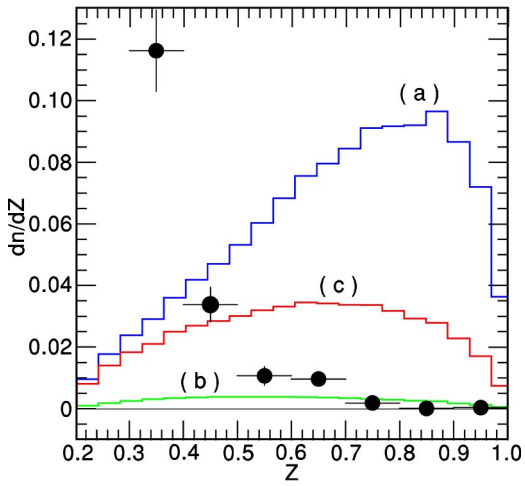

FIG. 9. The measured dn/dZ spectrum of $\Upsilon(1S)\to(ggg)\to\eta' X$ compared with theoretical predictions. Shown in dots are the measurement in this study. Shown in lines are different theoretical predictions: (a) a slowly falling form factor, (b) a rapidly falling form factor, and (c) intermediate form factor [8]. These predictions are valid only in the region $Z>0.7$.

Listed in Table IV are the differential branching fractions in Z intervals for $\Upsilon(1S)$ decays to η' for ggg and $q\bar{q}$ subsamples and all decays.

In the Z spectrum of η' mesons produced via ggg, there is an excess above an apparent exponential decrease for $0.6<Z<0.7$, corresponding to a recoil mass opposite the η' in the range 5.3 to 6.1 GeV [16]. However, a detailed study did not reveal any narrow structures. A possible explanation is that there is more than one process contributing to this distribution. We note also that the $q\bar{q}$ has much larger rates at high Z than ggg.

IV. COMPARISON WITH THEORY AND CONCLUSIONS

Figure 9 shows the Z spectrum of the η' measured in this paper compared with the spectra predicted by the three different models described above. The models are expected to dominate η' production only for $Z>0.7$, with other fragmentation based processes being important at lower Z. The measurement strongly favors a rapidly falling q^2 dependence of the $g^*g\eta'$ form factor predicted by perturbative QCD (PQCD) [9,10], and ruling out other models.

In conclusion, we have made the first measurement of the η' energy spectrum from $\Upsilon(1S)\to ggg$ decays. Our data are not consistent with an enhanced $\eta' g^* g$ coupling at large η' energies. Thus, the large observed η' yield near end point of the charmless B decay spectrum cannot be explained by a large $\eta' g^* g$ form factor. Therefore, new physics has not been ruled out and may indeed be present in rare b decays.

ACKNOWLEDGMENTS

We thank Alex Kagan for providing us with his calculations and A. Kagan and A. Ali for useful discussions on the theoretical models. We gratefully acknowledge the effort of the CESR staff in providing us with excellent luminosity and running conditions. M. Selen thanks the Research Corporation, and A.H. Mahmood thanks the Texas Advanced Research Program. This work was supported by the National Science Foundation and the U.S. Department of Energy.

[1] A.L. Kagan, Phys. Rev. D **51**, 6196 (1995); M. Neubert, "Heavy Flavour Physics," CERN-TH/95-307, hep-ph/9511409.

[2] Particle Data Group, K. Hagiwara *et al.*, Phys. Rev. D **66**, 010001 (2002).

[3] CLEO Collaboration, T.E. Browder *et al.*, Phys. Rev. Lett. **81**, 1786 (1998).

[4] They measure $\mathcal{B}(B\to\eta' X_s)=[6.8^{+0.7}_{-1.7}(\text{stat})\pm 1.0(\text{syst})^{+0.0}_{-0.5}(\text{bkg})]\times 10^{-4}$ in the η' momentum range between 2.0 and 2.7 GeV/c. See BABAR Collaboration, B. Aubert *et al.*, "Study of Semi-inclusive Production of η' Mesons in B Decays," SLAC-PUB-8979, hep-ex/0109034.

[5] D. Atwood and A. Soni, Phys. Lett. B **405**, 150 (1997).

[6] W.S. Hou and B. Tseng, Phys. Rev. Lett. **80**, 434 (1998).

[7] A.L. Kagan and A.A. Petrov, hep-ph/9707354; A. Kagan, in Proceedings of the "Seventh International Symposium on Heavy Flavor Physics," Santa Barbara, California, 1997, hep-ph/9806266.

[8] A.L. Kagan, in *Proceedings of the 9th International Symposium On Heavy Flavor Physics*, CalTech, Pasadena, California, 2001, edited by Anders Ryd and Frank C. Porter, AIP Conf. Proc. No. 618 (AIP, Melville, NY, 2002), p. 310; Y. Chen and A.L. Kagan, University of Cincinnati report (in preparation).

[9] A. Ali and A.Y. Parkhomenko, Phys. Rev. D **65**, 074020 (2002).

[10] T. Muta and M.-Z. Yang, Phys. Rev. D **61**, 054007 (2000).

[11] The ARGUS Collaboration had an integrated luminosity of 32 pb^{-1} on the $\Upsilon(1S)$ resonance. Kagan [8] cites the upper limit in the higher Z region $\mathcal{B}_{Z>0.7}(\Upsilon(1S)\to\eta' X)<(6.5\pm 1.3)\times 10^{-4}$, where he extracted the number from A. Zimmermann, diploma thesis, University of Dortmund, 1992, where no continuum subtraction was attempted. [See also, ARGUS Collaboration, H. Albrecht *et al.*, Z. Phys. C **58**, 1199 (1993).]

[12] CLEO Collaboration, R. Ammar *et al.*, Phys. Rev. D **57**, 1350 (1998).

[13] CLEO Collaboration, Y. Kubota *et al.*, Nucl. Instrum. Methods Phys. Res. A **320**, 66 (1992).

[14] CLEO Collaboration, W.Y. Chen *et al.*, Phys. Rev. D **39**, 3528 (1989).

[15] We use the ratio of integrated luminosities of $\Upsilon(1S)$ and off-resonance data in calculating $f_{e^+e^-\to q\bar{q}}$ and $f_{\Upsilon(1S)\to q\bar{q}}$. The uncertainty of this ratio is about $\pm 1\%$. The uncertainty of $\sigma_{\Upsilon(1S)\to\mu^+\mu^-}$, 4%, also affects $f_{\Upsilon(1S)\to q\bar{q}}$. These latter two directly affect the branching fraction in the $q\bar{q}$ sample with uncertainties of 1% and 4% respectively. The effects of these

two sources to the overall and the *ggg* sample branching fractions are negligible except for the branching fraction measurement of high energy η' in the *ggg* samples, where there are $\pm 2.9\%$ and $\pm 3.6\%$ uncertainties.

[16] We fit the Z distribution in the range $0.3<Z<1$, not including the point $0.6<Z<0.7$, to an assumed inherent exponential shape and determined that this point is 3.3 standard deviations in excess.